BUREAU OF MINERAL RESOURCES, GEOLOGY AND GEOPHYSICS

RECORD

Record 1980/64

CALCULATION OF SYNTHETIC SEISMOGRAMS BY THE REFLECTIVITY METHOD

by

Professor Karl Fuchs,
University of Karlsruhe, West Germany.

W O R K S H O P

on

CALCULATION OF SYNTHETIC SEISMOGRAMS BY THE REFLECTIVITY METHOD

Karl Fuchs, University Karlsruhe/West-Germany

held at the Bureau of Mineral Resources

Canberra, 8-9 October 1980

Contents

List of Figures.

Synthetics encourage to discover nature's hidden beauties

Ben Akiba

Abstract

This workshop will provide an introduction to the practical procedure of computing synthetic seismograms by the REFLECTIVITY METHOD. After a few historical comments and brief outline of the theoretical background, a detailed description will be given of those key parameters which govern the fidelity of the synthetic seismogram sections.

Three cases will be discussed where application of the reflectivity method provides additional information not obtainable from travel time analysis alone: Cerveny effect, bright cusp and tunnelling waves.

Exercises at the computer will be provided for the participants to practise their own judgement in the production of synthetic record sections.

1. Introduction to the Reflectivity Method

The REFLECTIVITY METHOD , developed by Fuchs (1968) and Fuchs & Müller (1971), recognises that observed record sections contain much more information than can be extracted using the classical inversion of travel-time data. In particular, at those points where information on the distribution of velocities is concentrated (e.g. at cusps) ray theory is only a very crude approximation.

The program REFLEXION has found a wide number of applications, including shallow and deep exploration seismic interpretation, crustal and upper mantle deep seismic sounding, the study of core/mantle to inner/outer core boundary for long period body waves, and other situations too numerous to be referenced here.

A number of authors have progressively improved the program REFLEXION, including - Kennett (1975b): inclusion of Q and of differing structures under source and receivers; Kind (1976): improvement in the computation of the reflectivity matrix; Kind (1978): inclusion of double-couple earthquake source into the reflecting medium at arbitrary depth; Stoffa et al. (pers. commun. 1980): considerable reduction in computer time by application of a hardware array processor; extension to 125 Hz for marine seismic work.

For details of the theoretical background, interested participants are referred to Fuchs (1968) and especially to Fuchs & Müller (1971). The Reflectivity Method is based on two concepts:

1) The response of a stack of horizontal, elastic layers to an incident harmonic wave of frequency ω and angle of incidence γ.

This can be computed by the well-known Thompson-Haskell matrix formalism (Haskell, 1953).

2) According to SOMMERFELD a spherical wave radiating from a point source can be decomposed into, or synthesized from, homogeneous plane waves radiating in all directions, plus a number of inhomogeneous waves travelling in a horizontal direction.

The potential function of a spherical compressional wave at some distance R from the source in a homogeneous medium:

$$\phi_0(v,z,t) = \frac{1}{R} \cdot F\left(t - \frac{R}{\alpha_1}\right) \qquad \ldots (1)$$

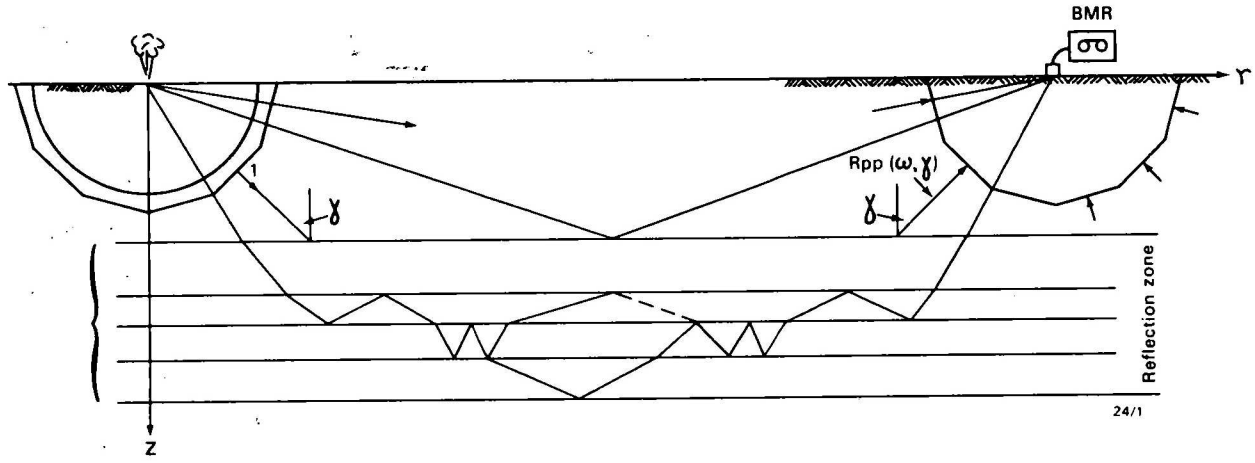

Fig 1. Point Source Response over layered medium

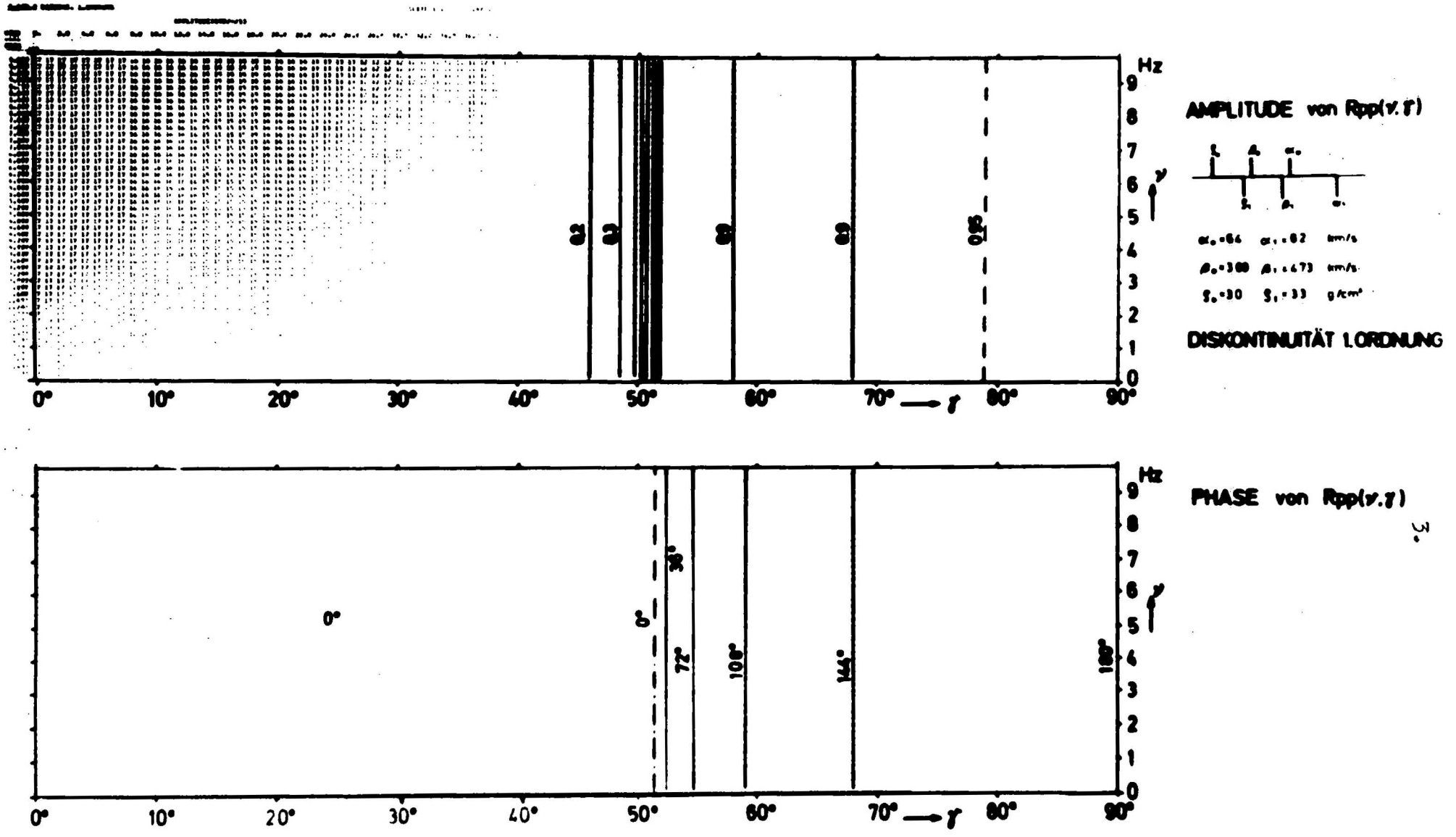

Figure 2 Reflectivity 1. Order discontinuity.

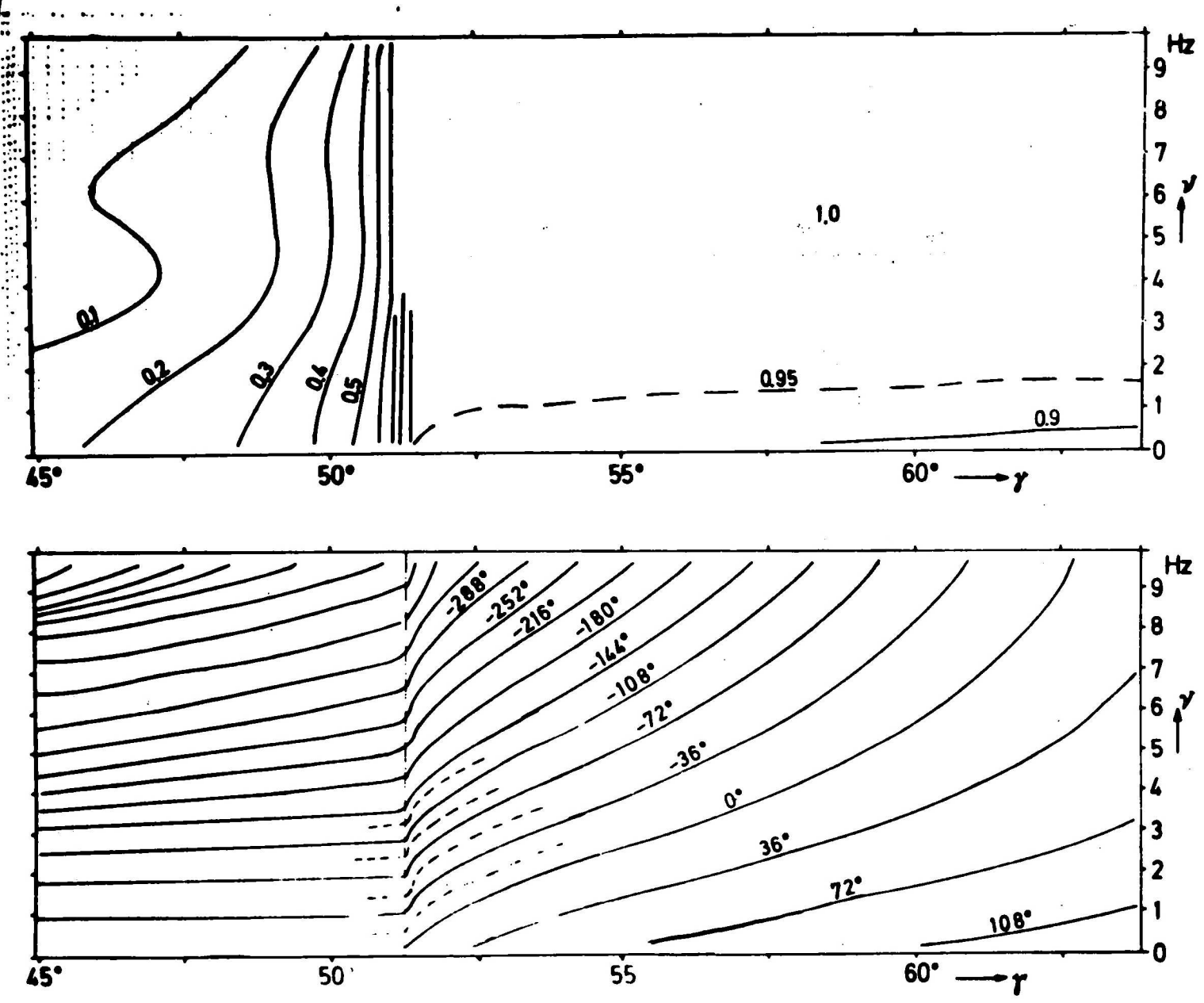

Figure 3 Reflectivity STEP + MOHO.

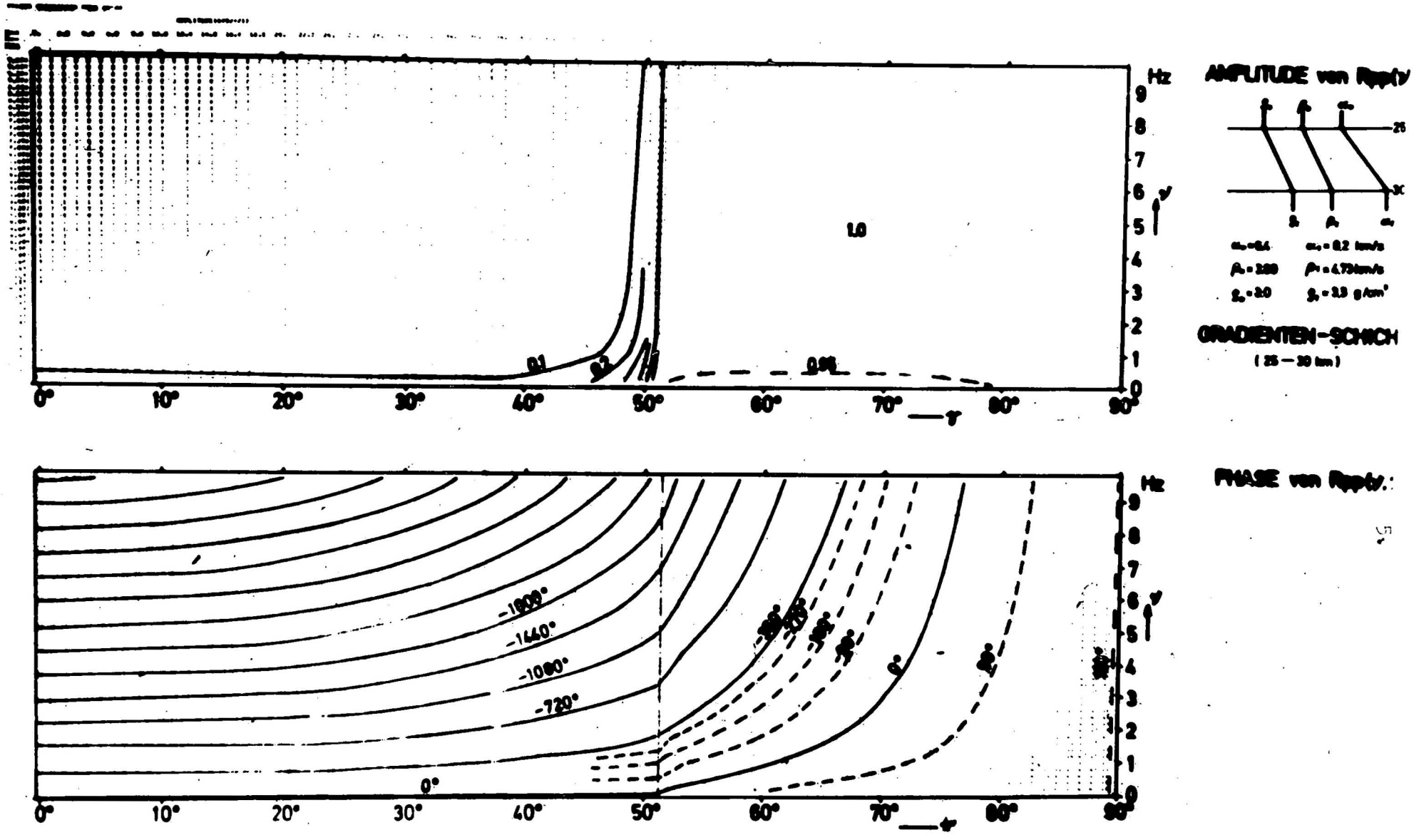

Figure 4 Reflectivity Transition zone.

can, after Fourier-Transformation according to Sommerfeld, be expressed as:

$$\tilde{\phi}_o(r,z,\omega) = \tilde{F}(\omega) \int_o^\infty \frac{k}{j\nu_1} J_o(kr) \cdot e^{-j\nu_1 z}\, dk \qquad (2)$$

where the integration is over all horizontal wave numbers

$$k = \frac{\omega}{c} = \frac{\omega}{\alpha_1} \cdot \sin\gamma \qquad (3)$$

and

$$\nu_1 = \left(k_{\alpha_1}^2 - k^2\right)^{\frac{1}{2}} \qquad (4)$$

is the vertical wave number. The decomposition into plane waves is more readily recognised if the large argument approximation for the J_o-Bessel function is introduction into (2):

$$J_o(x) = \frac{1}{\sqrt{2\pi x}} \left(e^{j(x-\frac{\pi}{4})} + e^{-j(x-\frac{\pi}{4})}\right) \qquad (5)$$

$$\tilde{\phi}_o(r,z,\omega) = \frac{F(\omega)}{\sqrt{2\pi}} \int_o^\infty \frac{1}{j\nu_1} \sqrt{\frac{k}{r}} \left[e^{j(kr-\nu_1 z-\frac{\pi}{4})} + e^{-j(kr+\nu_1 z-\frac{\pi}{4})}\right] dk \qquad (6)$$

Both terms I and II represent propagating waves in the negative z-direction, i.e. upward; I is propagating away from the source (pos r) while II is propagating towards the source. For all practical purposes the contribution of II is negligible.

Every one of these plane harmonous and homogeneous waves is reflected from the transition zone having undergone a change in amplitude and a phase shift, both expressed in the complex reflectivity function

$$\tilde{R}_{pp}(\omega,\gamma)$$

This is due to the interference of all possible multiple reflections and converted waves, and depends on the frequency ω and the angle of indicence γ.

No ray path or number of multiples has to be specified.

To obtain the response at a receiver at distance r from the source, the plane waves have to be multiplied by the corresponding reflectivity. Allowance must be made for the transmission through the overburden on its way down and up through the various interfaces and for the effect of the free surface. The final expression for the vertical displacement at the free surface is (z = 0):

$$\tilde{W}(r,0,\omega) = \tilde{F}(\omega)\int_0^\infty k \cdot J_0(kr)\, P_d \cdot \tilde{R}_{pp} \cdot P_u \left(1 - r_{pp} + \frac{k}{j\nu_1} \cdot r_{ps}\right) \cdot e^{-2j\sum_{i=1}^{m} h_i \nu_i} \cdot dk \qquad (7)$$

m = No. of layers in overburden.

P_d and P_u are the products of transmission coefficients at the interfaces passed by the ray on its way through the overburden. The exponential term takes care of the delay or phase shift during this travel. The expression in brackets is the effect of the free surface due to the P and S wave reflected here.

A characteristic feature of the method is the change of the variable of integration from wave number k to the angle of incidence γ at the top of the reflecting layer:

$$k = \frac{\omega}{c} = \frac{\omega}{\alpha_m} \cdot \sin\gamma = k_{\alpha_m} \cdot \sin\gamma \qquad (8)$$

With this transformation the products of the transmission coefficients, P_d, P_u, and the reflection coefficients at the free surface, r_{pp} and r_{ps}, depend only on angle of incidence γ. With this (7) becomes:

$$\tilde{W}(r,0,\omega) = \tilde{F}(\omega)\, k_{\alpha_m}^2 \int_{\gamma_1}^{\gamma_2} \sin\gamma \cdot \cos\gamma \cdot J_0(k_{\alpha_m} r \sin\gamma)\, \tilde{R}_{pp}(\omega,\gamma)\, H(\gamma) \cdot e^{-2jk_{\alpha_m}\sum_{i=1}^{m} h_i \eta_i} \cdot d\gamma \quad \ldots(9)$$

(for details of the expressions see Fuchs & Müller (1971)).

Integration from $k_1 = 0$ to $k_2 = \infty$

becomes $\gamma_1 = 0$ to $\gamma_2 = \frac{\pi}{2} + i\infty$

For the computation of synthetic seismograms for body waves it is, in general, sufficient to restrict the range of integration of $\gamma_1 = 0$ (vertical incidence) to $\gamma_2 = \frac{\pi}{\lambda}$ (grazing incidence at the top of the reflection zone) or even smaller ranges (see Fig.5).

Kind (1979) pointed out that the transformation from k to γ, and the use of equally spaced angles of incidence for the numerical integration, corresponds to a non-equally spaced distribution in the distance domain which Kind suggests might be the reason that no aliasing problems arose during the Bessel-transformation from k to distance domain.

In summary

To integrate numerically the complex reflectivity $\tilde{R}_{pp}(\omega, \gamma)$ has to be computed

- over a range of angles of incidence $< \gamma_1 , \gamma_2 >$
- at discrete angles γ_1 with an increment $\Delta\gamma$
- over a range of frequencies $< f_1 , f_2 >$
- at discrete frequencies ω_1 with an increment $\Delta\omega$

If $N_a = \frac{\gamma_2 - \gamma_1}{\Delta\gamma}$ is the number of angles

and $N_f = \frac{f_2 - f_1}{\Delta f}$ is the number of frequencies for which the Reflectivity has to be computed; then in total a number of

$$\boxed{N_a \cdot N_f} \text{ values of } \tilde{R}_{pp}(\omega, \gamma)$$

have to be computed and stored. This takes a considerable proportion of the computing time.

The beauty of the reflectivity method is that, once the reflectivity values have been computed, they are the same for an arbitrary number of distances. In (9) only the argument of the Bessel function is dependent upon distance. Therefore, with comparatively little effort, seismograms can be computed at an arbitrary number of distances.

2. Key Parameters and How they Influence Computer Time and Fidelity of Record Sections

Computation of synthetic seismograms with the reflectivity method provides high fidelity but can become quite expensive in terms of computer time. Therefore it is desirable to manipulate certain parameters in the process to minimise computer time and, at the same time, preserve the fidelity of the main features in the response seismogram.

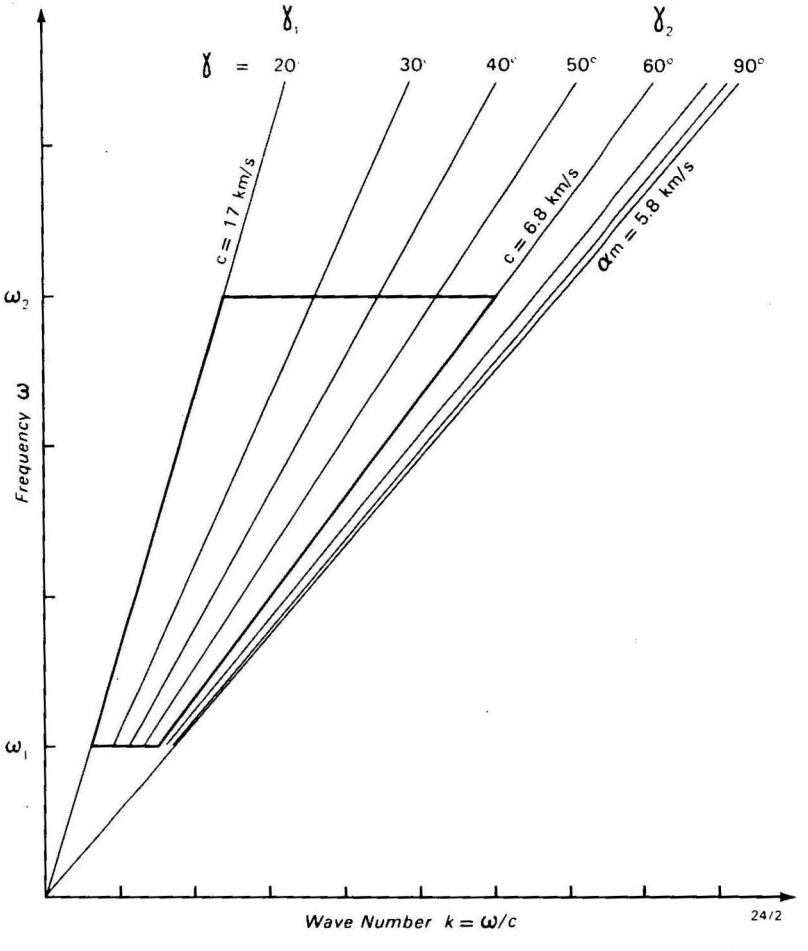

Fig 5. Frequency — Angle window

These manipulations may be divided into two main groups:

A) Manipulation of parameters concerning frequency, duration, angle of incidence (wave number)

B) Manipulation with the definition of the reflecting zone.

These are the key parameters of type A:

1. Δt: Time increment in the digital source signal and also in the time series of the response seismogram
2. T: Duration of the response time series
3. $< f_1 , f_2 >$: Frequency window
4. $< c_1 , c_2 >$: Phase velocity window
5. $\Delta\gamma$: Increment of angle of incidence

The manipulation of type B parameters concerns:

1. Definition of overburden layers and layers in the reflecting zone
2. Modelling transition layers
3. Flat earth approximation

All these manipulations will be discussed in detail in the following sections.

2.1 Time increment

The program REFLEXION allows the use of a series of built-in digital source signals with variable parameters controlling duration, number of cycles and dominant frequency. However, external digital signals can also be read in if it is felt that they better match the observed record section.

The choice of the increment Δt in either form is governed by two considerations:

a) Δt must be small enough to ensure that the amplitude spectrum of the source signal has effectively disappeared at the Nyquist-frequency

$$f_{N_y} = \frac{1}{2\,\Delta t}$$

to avoid aliasing.

b) Usually we use a much smaller Δt, shifting the Nyquist-frequency well beyond any contribution of the source spectrum

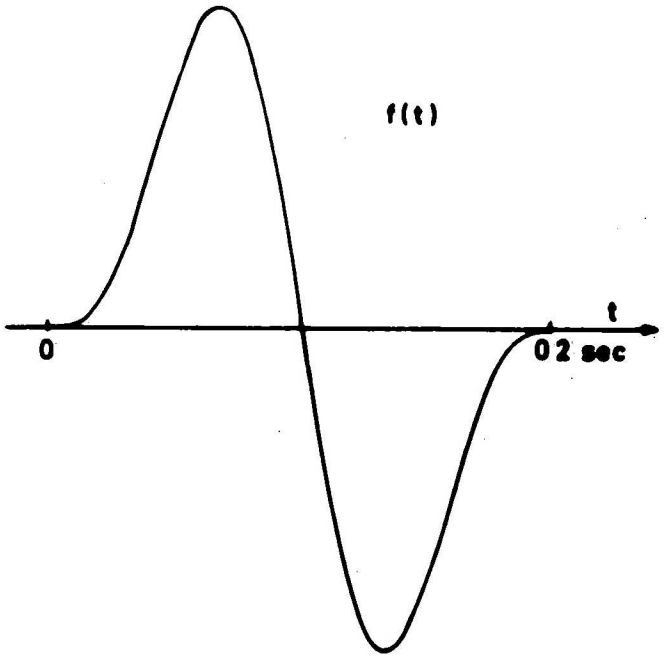

$$f(t) = \begin{cases} \sin 10\pi t - \frac{1}{2}\sin 20\pi t & \text{für } 0 \leq t \leq 0.2 \text{ sec} \\ 0 & \text{für } t<0 \text{ und } t>0.2 \text{ sec} \end{cases}$$

Einfallendes Signal f(t)

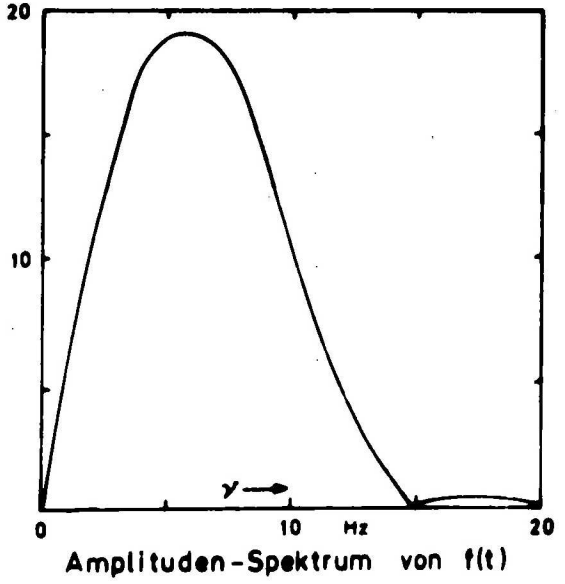

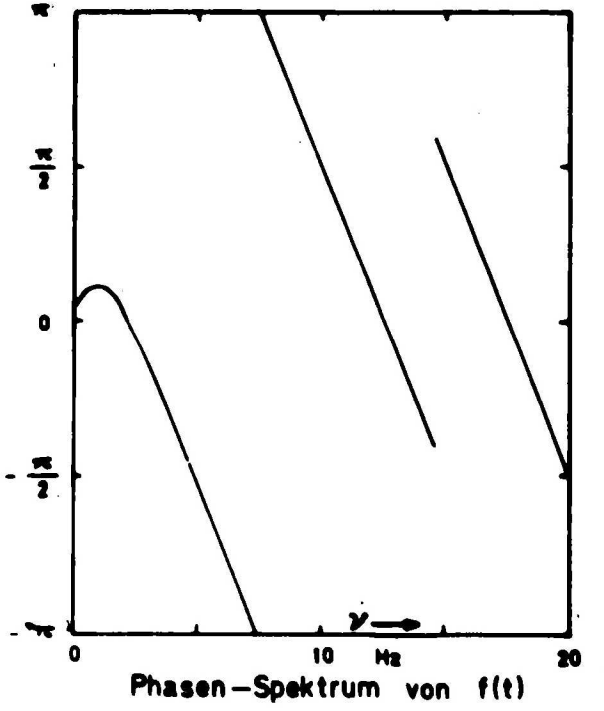

Figure 6 Source Signal + Spectrum.

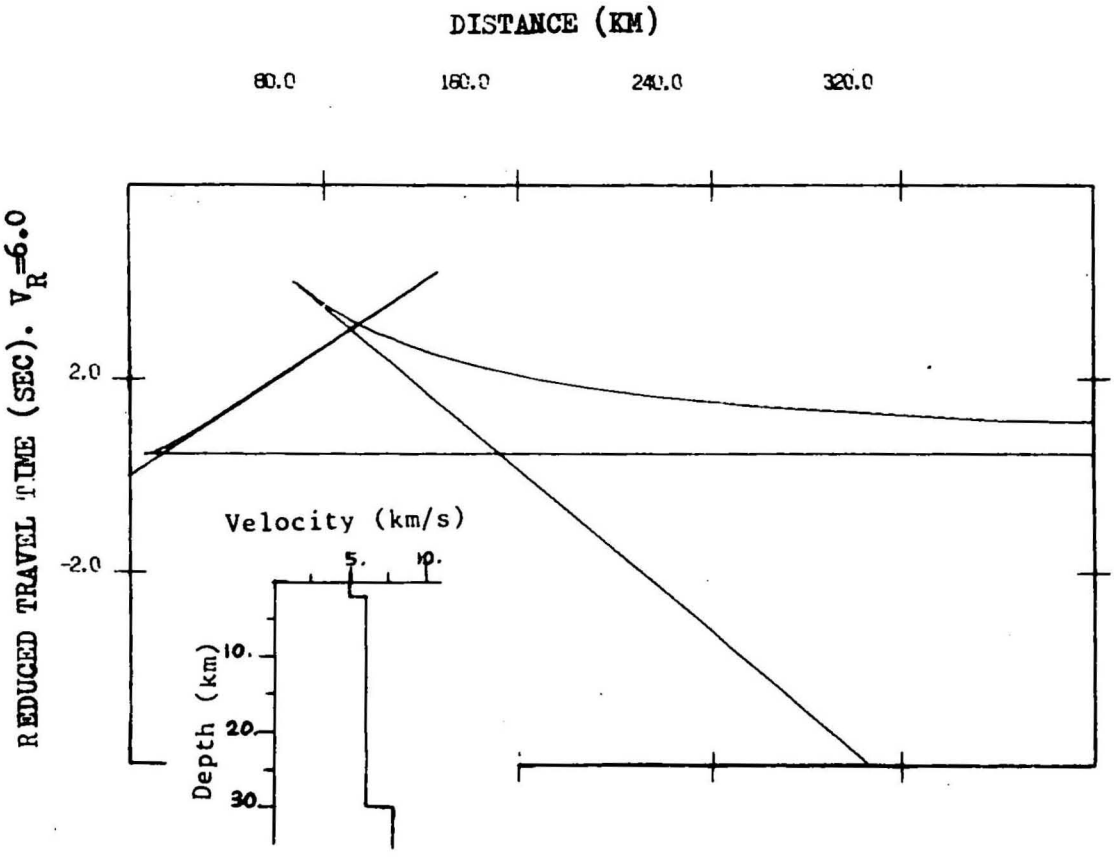

(a) Three Layer Model: V_1= 5.0, V_2= 6.0, V_3= 8.0 km/sec

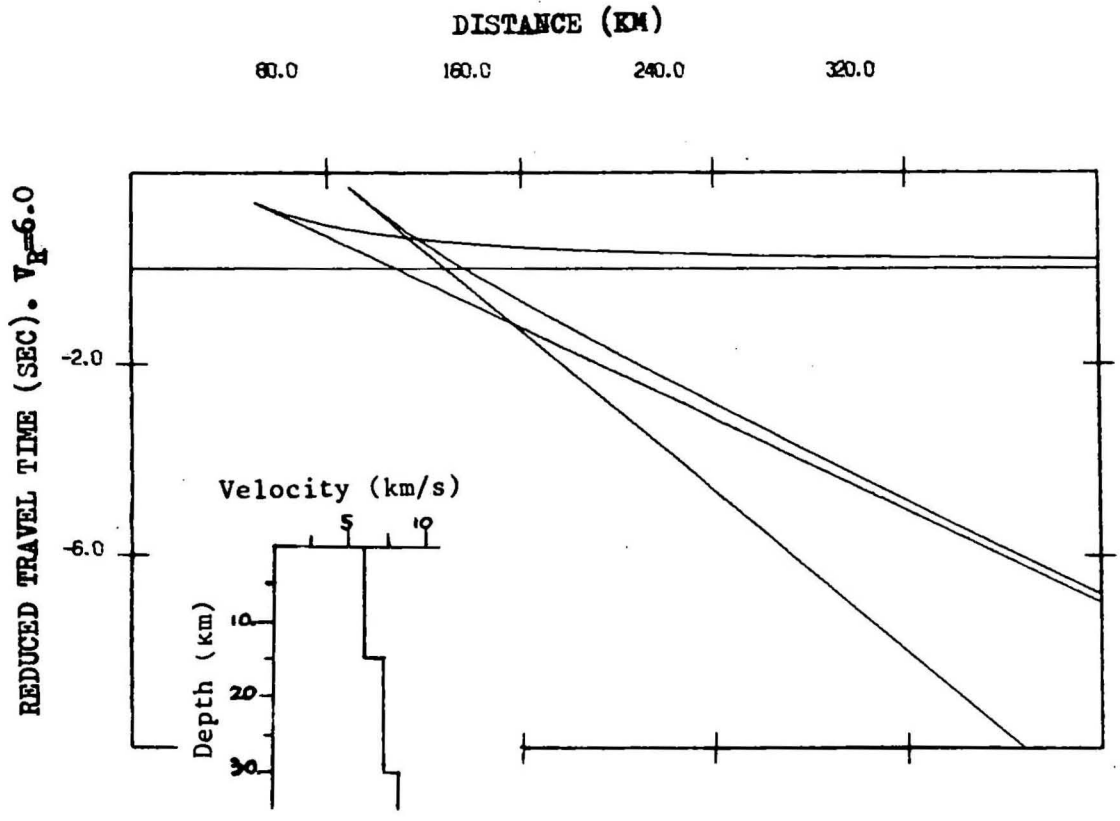

(b) Three Layer Model: V_1= 6.0, V_2= 7.0, V_3= 8.0 km/sec

Figure 7 Three layer travel time curve & model.

It will be shown in section 2.3 on the frequency window that this extension of the Nyquist-frequency does not increase the computer time as long as the reflectivity is only computed in the pass-band of the source signal.

The choice of a smaller Δt smoothes the response time series at negligible additional cost .

2.2 Duration of response time series

Consider the travel-time curves of a rather simple 2 layer crust over a homogeneous half space (Fig. 7). These travel-time curves already give a rough idea about the kind of seismograms to be expected from a given layered model. We know the locations of the points of interest in time and distance.

- cusps of triplications
- critical distances
- crossover distances

What we do not know from travel-time computations are:

- decay of amplitude with distance
- deformation of signals near cusps
- relative amplitudes between various branches
- other deviations of wave theory from geometrical ray theory

Even in this simple case computer time may increase considerably if we do not take certain precautions. Before a synthetic seismogram or a record section in a certain distance range is computed we must decide which is the longest response time in our record section. By response time we mean the actual duration in time of a P-wave seismogram "recorded" at a certain distance. This response time depends very much upon distance. Near the cross-over it can be rather short; as P_g and P_n diverge with larger distance it can become intolerably large.

In later sections we will discuss some means of reducing the response time artifically. But in this section we will show, for the simplest case of a 1st-order discontinuity, what may happen if the response time is chosen incorrectly.

The record section produced by REFLEXION may be computed with an arbitrary reduction velocity VRED starting at an arbitrary time T_o. Usually T_o should be chosen in such a way that the reduced times of the first arrivals follow shortly after T_o.

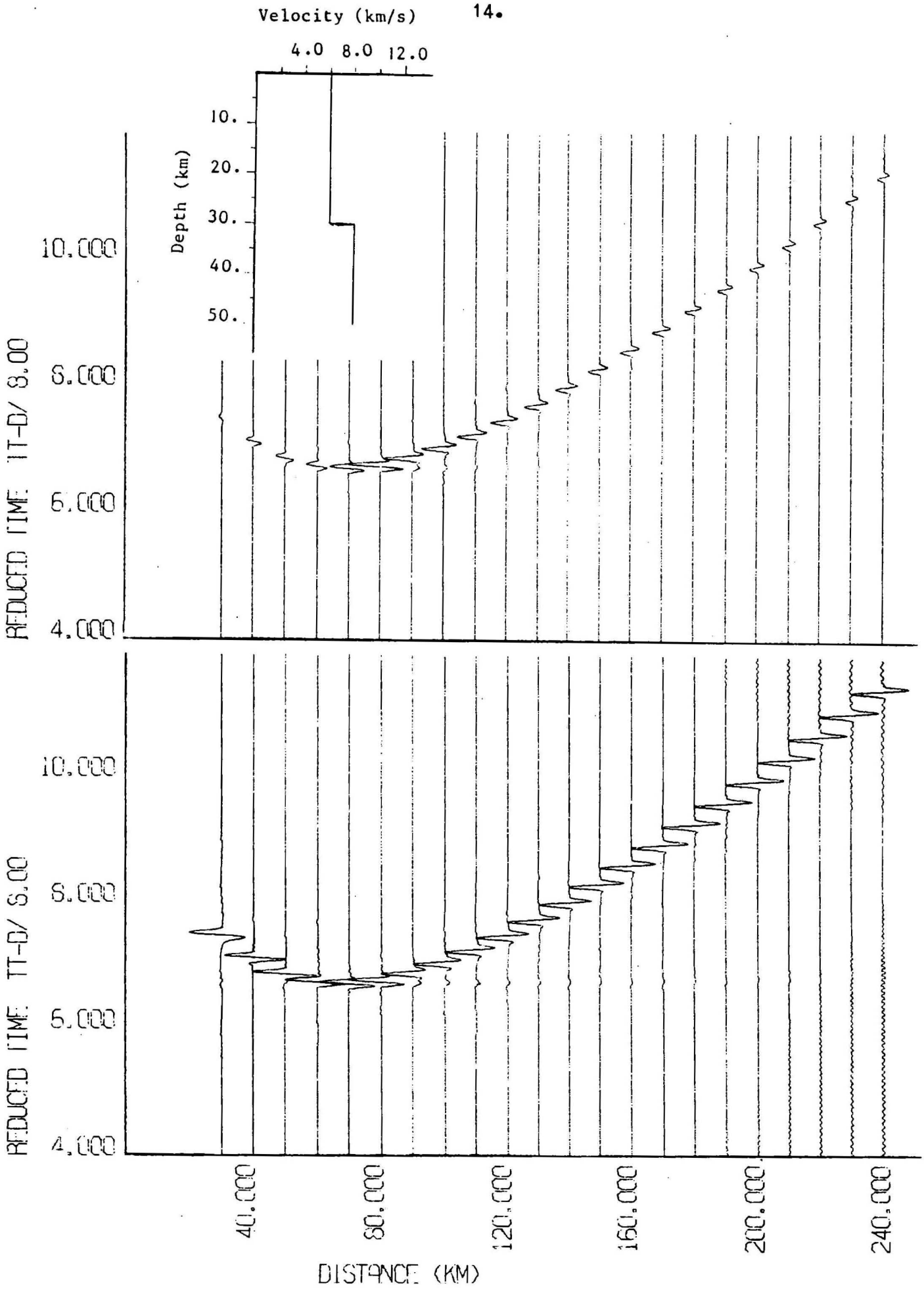

Figure 8 Record section 1. order discontinuity.

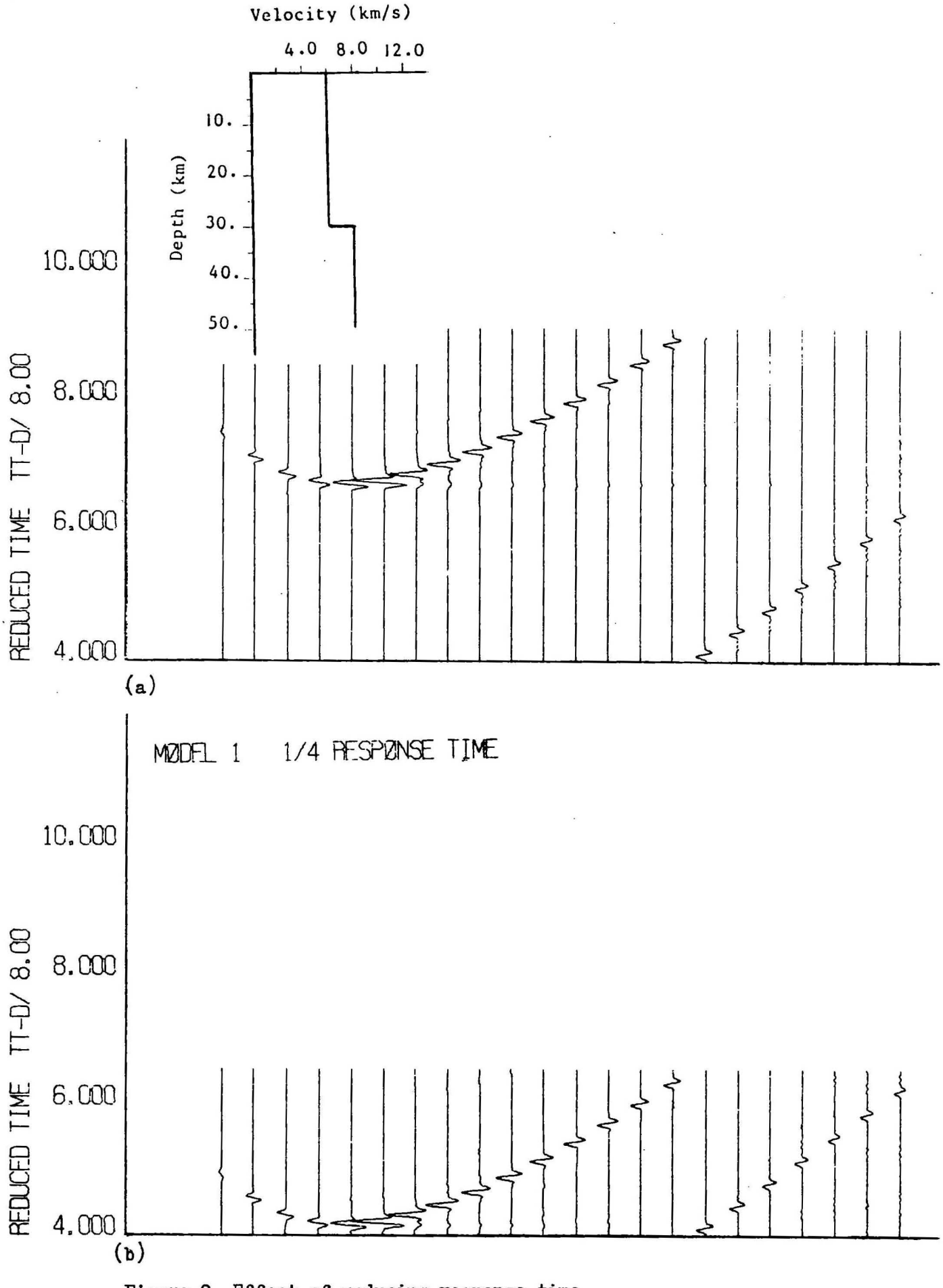

Figure 9 Effect of reducing response time.

Fig. 8 gives the synthetic record sections for a first-order discontinuity. The chosen duration is 10.24 s; it is the same for all distances, and all phases (PmP and Pn) fit into the T-D-frame.

In Fig. 9a and b the duration of the response has been purposely set to $\frac{1}{3}$ or 1/4, respectively of that selected in Fig. 8.

Although the response time is now too short the PmP signal which does not fit into the time frame appears at the beginning of the record section. This becomes even more apparent in Fig. 9b and may lead to strong interference and signal deformation.

This phenomenon is aliasing in the time domain when a discrete spectrum is Fourier transformed with too large frequency increment 1/T' where T' is the "Nyquist-time" which should be larger than the actual response time. The response is periodic in the time domain and folds into neighbouring domains.

Although it is essential to reduce the response duration as much as possible, care should be taken that phases (perhaps even not thought of before) do not fold into the record section, and, especially, that they do not interfere.

2.3 Frequency window

The number of frequencies is essentially determined by the selection of the time increment Δt and the duration T of the response. The Nyquist-frequency is

$$f_{Ny} = \frac{1}{2\Delta t}$$

and the frequency increment

$$\Delta f = \frac{1}{T} = \frac{1}{\Delta t \,.\, NPTS}$$

where NPTS is the number of points in the response time series.
Therefore, the number of frequency points up to the Nyquist frequency is

$$N_{FNy} = \frac{f_{Ny}}{\Delta f} = 0.5 \,.\, NPTS$$

(Remark: the reflectivity is only computed up to the Nyquist frequency; the contributions above are complex conjugate to those below the Nyquist-frequency).

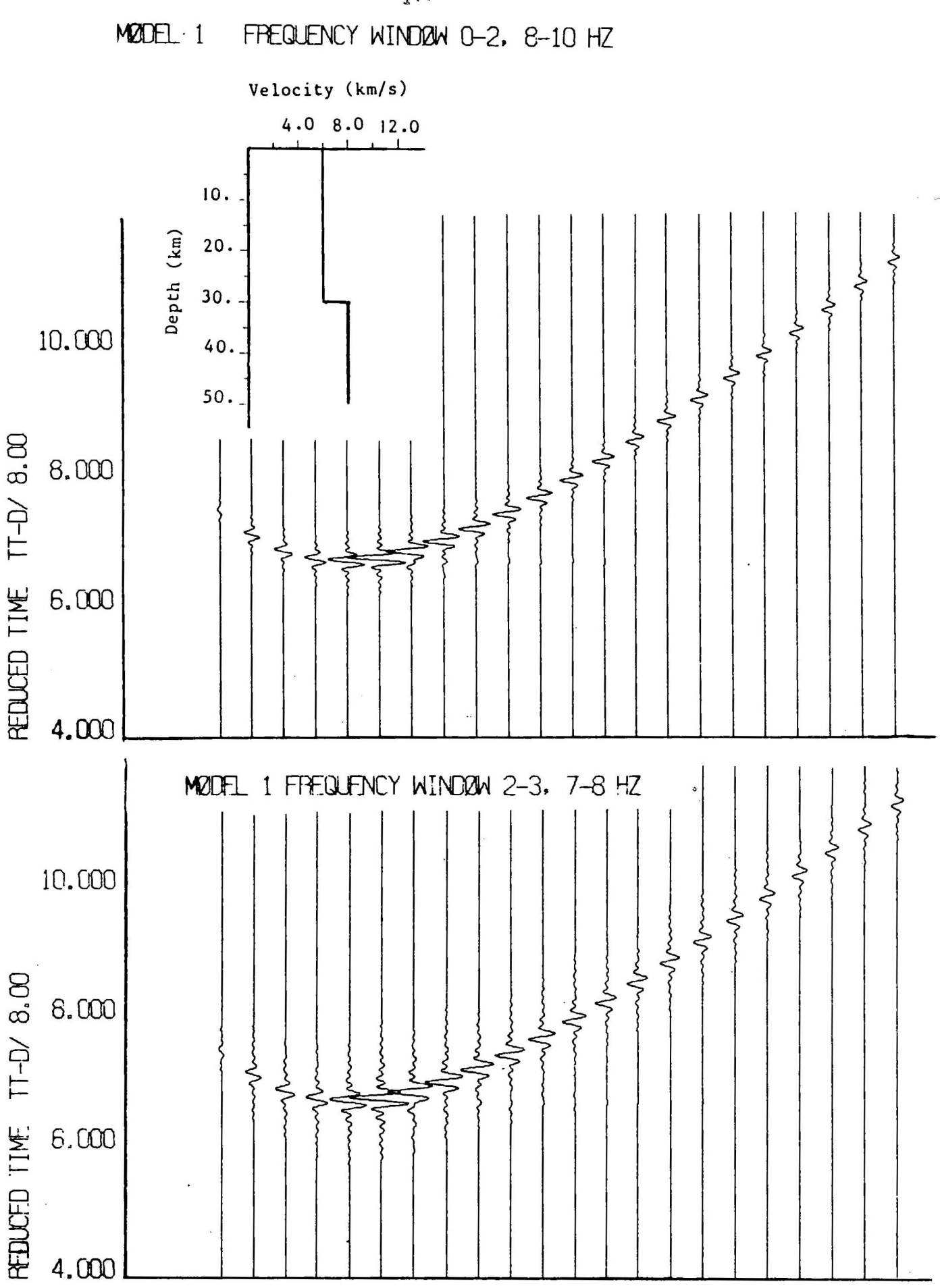

Figure 10 Effects of various frequency windows.

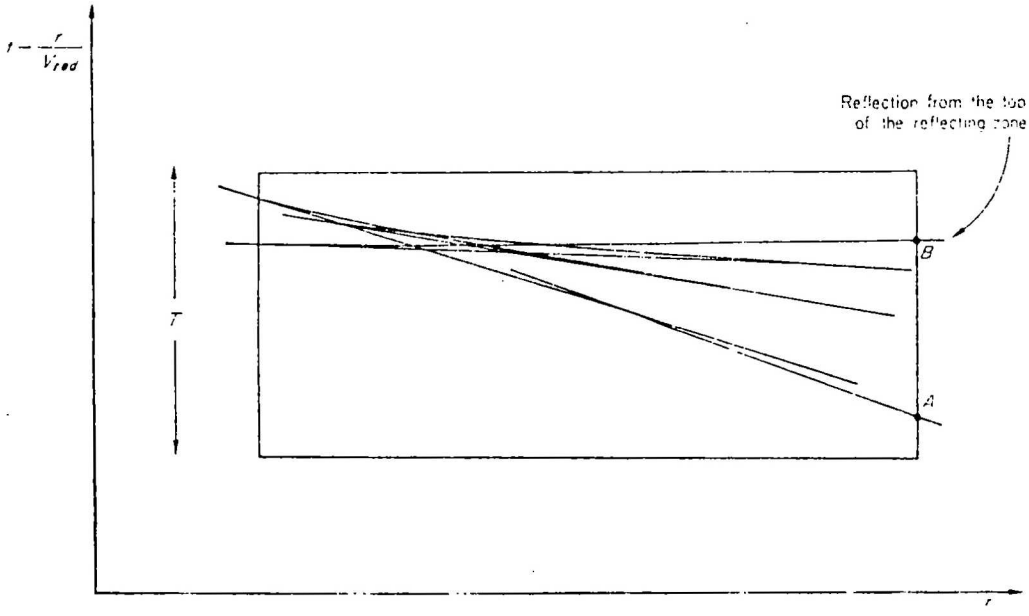

Reduced travel time diagram for the reflecting zone of an arbitrary model.
It is assumed that theoretical seismograms are to be computed inside the rectangle.

Figure 11 Selection of velocity window.

However, as mentioned in section 2.1, Δt is usually chosen much smaller than is required by the frequency pass-band of the signal. The Nyquist-frequency f_{Ny} is much larger than the upper frequency limit f_2 of the source signal. If its lower frequency is f_1, we are dealing with a bandwidth (f_2-f_1) of the frequency window. The number of frequency steps Δf in this window is

$$N_F = \frac{f_2 - f_1}{\Delta f} = (f_2 - f_1) \,.\, \Delta t \,.\, NPTS$$

In other words:

Number of frequency values = Bandwidth * Duration i.e. the number N_F of frequencies does not depend on the number NPTS in the response time series, but only on its actual duration.

There is no saving in computer time in the attempt to reduce the number of data points NPTS in the response time series by an increase in Δt, because, according to this equation, the number of frequencies at which the reflectivity has to be computed is not dependent upon NPTS, but only upon the product NPTS.Δt.

The only way to save computer time in the number of frequencies for which reflectivity values are computed is by a careful narrowing of the passband $(f_2 - f_1)$. Smoothing with cosine-windows should, and can, be applied to avoid corner effects.

2.4 Phase velocity window

In section 1. it was explained that, in the reflectivity method, integration over wave number k is replaced by integration over angle of incidence γ at the top of the reflection zone. Every angle of incidence corresponds to a certain horizontal phase velocity c:

$$c = \alpha_m / \sin\gamma$$

where α_m is the P-velocity in the layer directly on top of the reflection zone. For body waves, the range of integration of γ is $< 0; \pi/2 >$ i.e. the phase velocities c vary in the range $< \infty; \alpha_m >$. Although theoretically all these phase velocities, ranging from vertical to grazing angle of incidence, contribute to the response at every distance, it is evident from a time-distance plot that in the time-distance range of interest the range of phase velocities is restricted (Fig. 11). In a distance range where no subcritical reflections are to be expected, the maximum phase velocity c_1 would

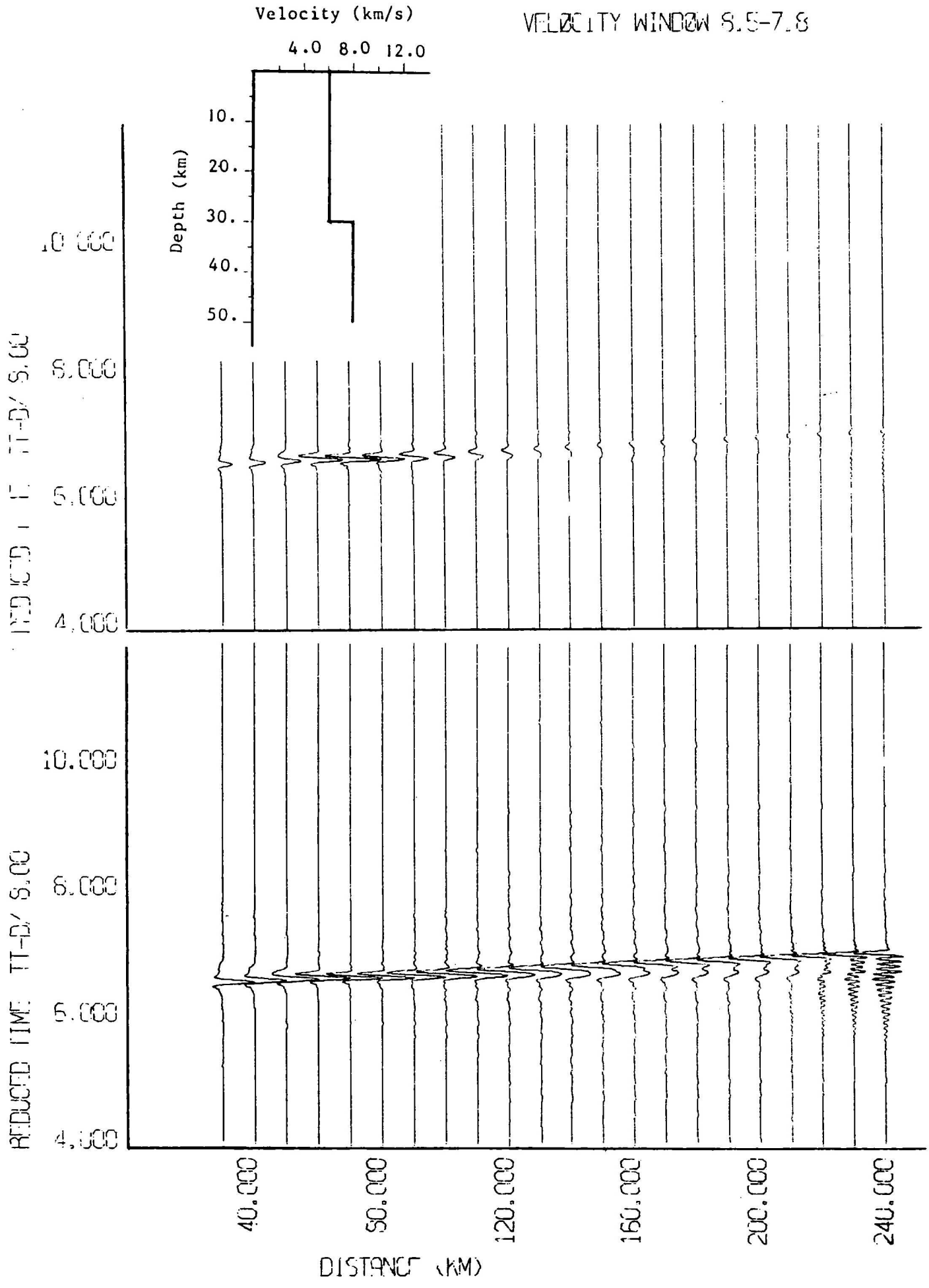

Figure 12 Spurious signals due to velocity cut-offs.

be the fastest velocity in the reflecting zone, and the slowest c_2 the velocity α_m in the layer directly on top of the reflecting zone. The corresponding angles of incidence are:

$$\gamma_{1,2} = \sin^{-1} \frac{\alpha_m}{c_{1,2}}$$

The minimum phase velocity c_2 must be chosen larger than the maximum velocity in the overburden. For a study of the super-critical reflections from the top of the reflecting zone at large distances, c_2 should be chosen as close as possible to this maximum velocity in the overburden, e.g. +0.002 km/sec. (The program will exit with an error message if c_2 is chosen less than the maximum overburden velocity).

In sub-critical reflections are to be included into the synthetic record section, the maximum phase velocity must be increased at least to the maximum phase velocity encountered on the reflection branches. However, to assure fidelity of amplitudes it is recommended that the specified maximum phase velocity be a good deal higher than the actual maximum phase velocity in the range of interest. Even for the study of the amplitudes of a P_R-phase with a velocity of 8.2 km/s, the upper velocity c_1 should be set to at least 10 km/sec.

The narrowing of the velocity window $\langle c_1, c_2 \rangle$ can save considerable computer time. If applied with care the fidelity of amplitudes and signal shape is preserved. However, application of this velocity-filter (that is what the velocity-window amounts to) causes the appearance of spurious signals travelling with the two cut-off phase velocities, usually folding back into the selected time-distance range of the record section as soon as they reach the margin. They start at those points of the travel time curves where these cut-off phase velocities are encountered (Fig. 12). The amplitudes of these spurious phases are proportional to the amplitudes of the reflected wave field at those points where these spurious phases originate. Their amplitudes can be diminished to a certain degree by applying various forms of smoothing windows.

2.5 Increment of angle of incidence

After the definition of the phase velocity window $\langle c_1, c_2 \rangle$ which corresponds to a window of angle of incidence $\langle \gamma_1, \gamma_2 \rangle$, the choice of the increment $\Delta\gamma$ in the angle of incidence for the numerical integration of equation (9) determines the number of N_a of angles at which the reflectivity has to be computed given a certain frequency.

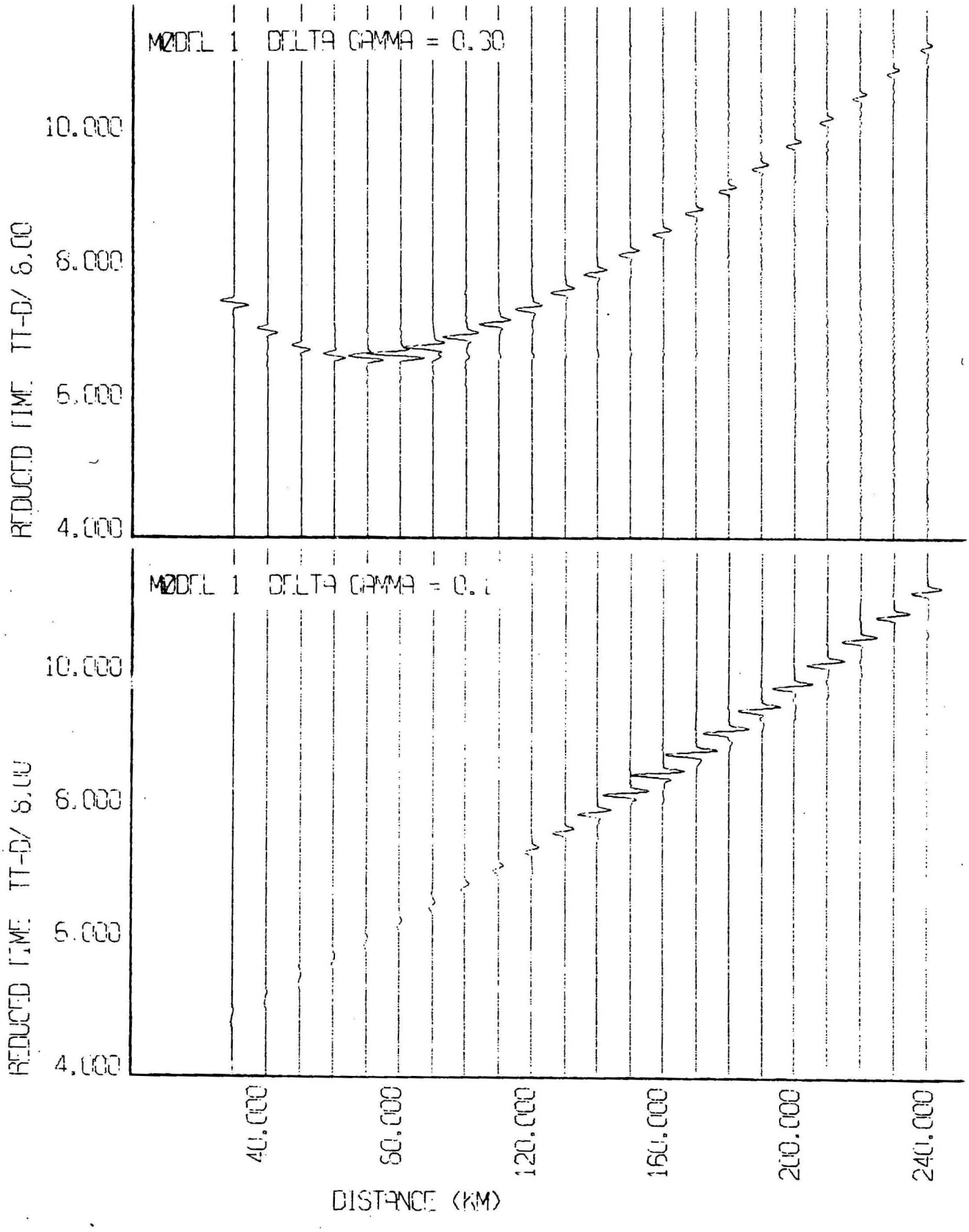

Figure 13 Effects of angle increments $\Delta\gamma$.

Up to now increments $\Delta\gamma$ between 0.05° and 0.5° have been used. The most frequently used value is 0.25°.

Larger values of $\Delta\gamma$ lead to considerable numerical noise (Fig. 12) which may completely mask the "true" reflected wavefield. This must be due to a modified form of aliasing in the distance domain during the Fourier-Bessel transformation from wave-number to distance.

The number of angles of incidence at which reflectivity values have to be computed for every frequency is

$$N_a = (\gamma_2 - \gamma_1)/\Delta\gamma$$

2.6 Example for number of reflectivity values to be computed

Duration of seismogram response:	$T = 5.12$ sec
Bandwidth of signal:	$(f_2 - f_1) = 9.77$ Hz
Angle window (open):	$(\gamma_2 - \gamma_1) = 90°$
Increment of angle:	$\Delta\gamma = 0.25$; (0.1°)

The total number N of reflectivity values to be computed is

$$N = [\text{Duration } T] \times [\text{Bandwidth } (f_2 - f_1)] \times [\text{Aperture } (\gamma_2 - \gamma_1)] / \Delta\gamma$$
$$= 5.12 \cdot 9.77 \cdot 90/0.25$$
$$= 18000; \quad (45000)$$

2.7 Saving computer time by definition of overburden layers and reflection zone layers

The REFLEXION- program comprises a feature which enables considerable saving of computer time in two ways. The stack of homogeneous layers which forms the model of the Earth's investigated layers is divided into two categories:

1) Overburden layers,
2) Reflecting zone layers

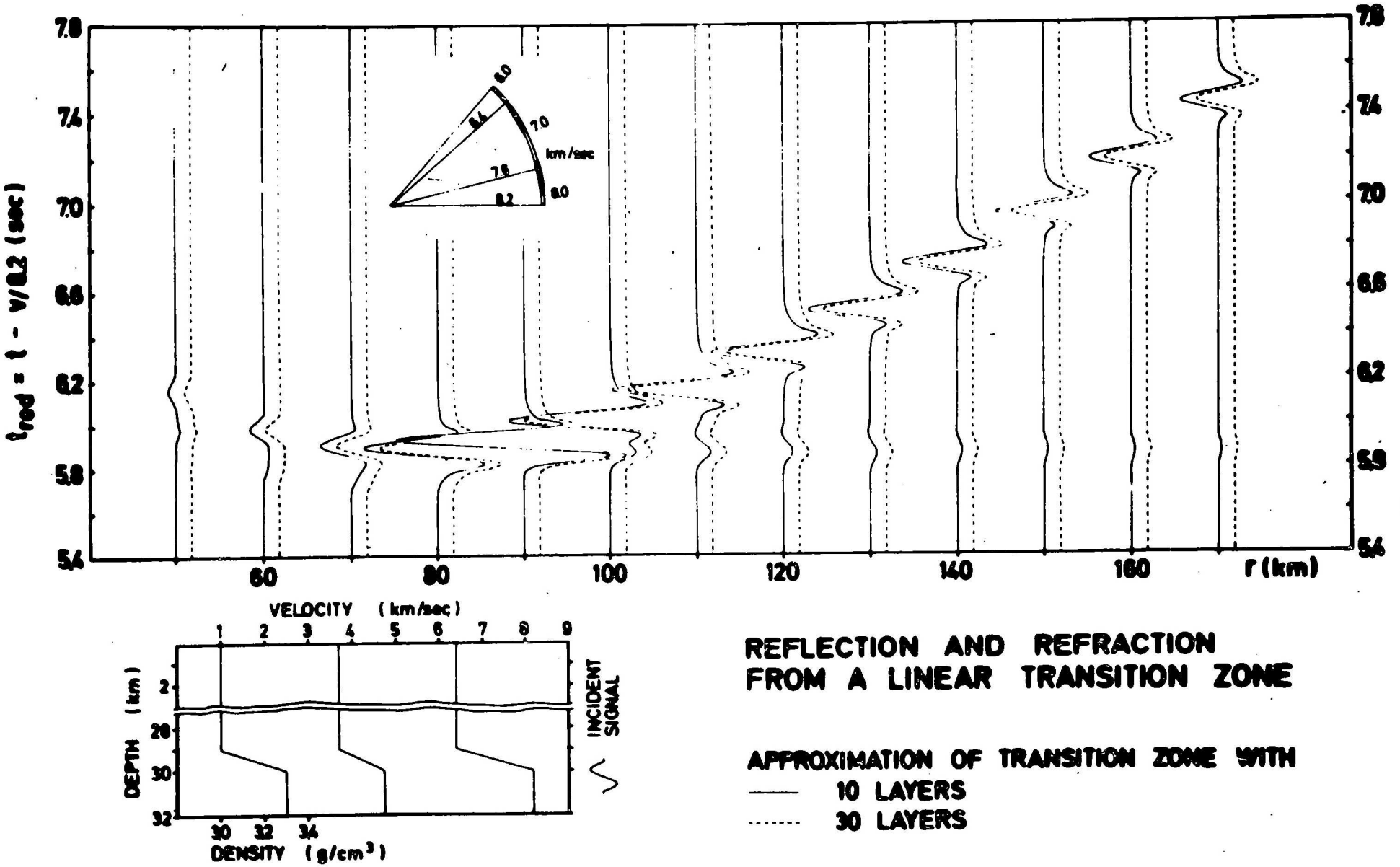

Figure 14 Modelling transition zones.

By a simple change of code all or some lower part of the overburden may be included in the reflecting zone. Alternatively, the top layers of the reflecting zone may be declared to belong to the overburden.

At the beginning of the comparison of observed and theoretical seismograms it would be a waste of computer time to calculate the complete response of all layers of the model. Instead, modelling can begin with the prominent branch of the shallow layers and exclude the deeper layers from the calculation. Computer time is not only saved by fewer layer matrices having to be multiplied for the reflectivity, but also because the response time can become noticeably shorter by working on single branches of the total reflected wave field.

Proceeding from the modelling of the shallow layer branches, the "deeper" branches are modelled one after the other as single units. The layers which produce the "shallower" branches are declared to be overburden and therefore do not enter the reflectivity calculation or contribute to the response time.

Only in the last step, when all branches have been modelled separately, is the complete response of the whole stack of layers in the model computed, and the relative amplitudes of the various branches compared and adjusted.

2.8 Modelling transition layers

Although the computation of the reflectivity $\tilde{R}_{pp}$ is based on the Thompson-Haskell matrix calculation for a stack of flat homogeneous horizontal layers, the REFLEXION algorithm has, since its introduction, also been applied to various forms of transition layers. This has been done in such a way that the transition zone is modelled by a stack of thin homogeneous layers with little velocity contrast. Should there be doubts whether a subdivision is fine enough or not, the thickness of the layers constituting the transition zone was halved and its number doubled. Fig. 14 is an example for such a test of a linear transition zone at the Mohorovičić discontinuity. The transition is subdivided into 10 and into 30 thin layers. The response is identical to within 3-4 digits. Therefore the smaller number of layers can be regarded as a sufficient approximation of the liner transition zone in this frequency band (0-10 Hz). As a rule of thumb, the velocity jumps should be not larger than 0.2 km/sec. However, this also depends very much on the dominant frequency of the signal. No firm rules have been established as yet.

2.9 Earth flattening approximation

In the program REFLEXION the algorithm to compute the reflectivity by the Thompson-Haskell matrix formulation is based upon flat homogeneous layers. The sphericity of the earth can normally be neglected in crustal explosion seismic work to a depth of about 30 km.

The reflectivity method has been applied however to much larger depths, e.g. Müller (1973) computed synthetic seismograms for long period body waves from the inner/outer core boundary. For this he developed an "Earth Flattening Approximation" (EFA; Müller, 1977) by which the spherical earth model is transformed into a model with flat inhomogeneous layers. The transformation is done in such a way that the time-distance curves computed in the inhomogeneous model are identical to those over the spherical earth model. This is achieved by increasing the velocity at a particular depth so as to compensate for the curvature of the spherical model.

If z, Vp, Vs, ρ are the values of depth, P-, S-velocity and density in the spherical earth model, the corresponding transformed values in the flat earth approximation are:

$$\bar{z} = 6370 \cdot \ln \frac{6370}{6370-z}$$

$$V_p(\bar{z}) = \frac{6370}{6370-z} \cdot V_p(z)$$

$$V_s(\bar{z}) = \frac{6370}{6370-z} \cdot V_s(z)$$

$$\rho(\bar{z}) = \left(\frac{6370}{6370-z}\right)^{NRH} \cdot \rho(z) \qquad 0 \leq NRH < 1$$

These inhomogeneous layers in turn have to be approximated again by a stack of thin homogeneous layers as described in the previous section 2.8.

3. Wave phenomena modelled with the reflectivity method

To a certain degree amplitudes of seismic waves can be calculated quite accurately from geometrical ray theory if geometrical spreading and energy splitting at interfaces is taken into account. However geometrical ray theory breaks down at those points where strong interference phenomena occur. Three examples will be discussed.

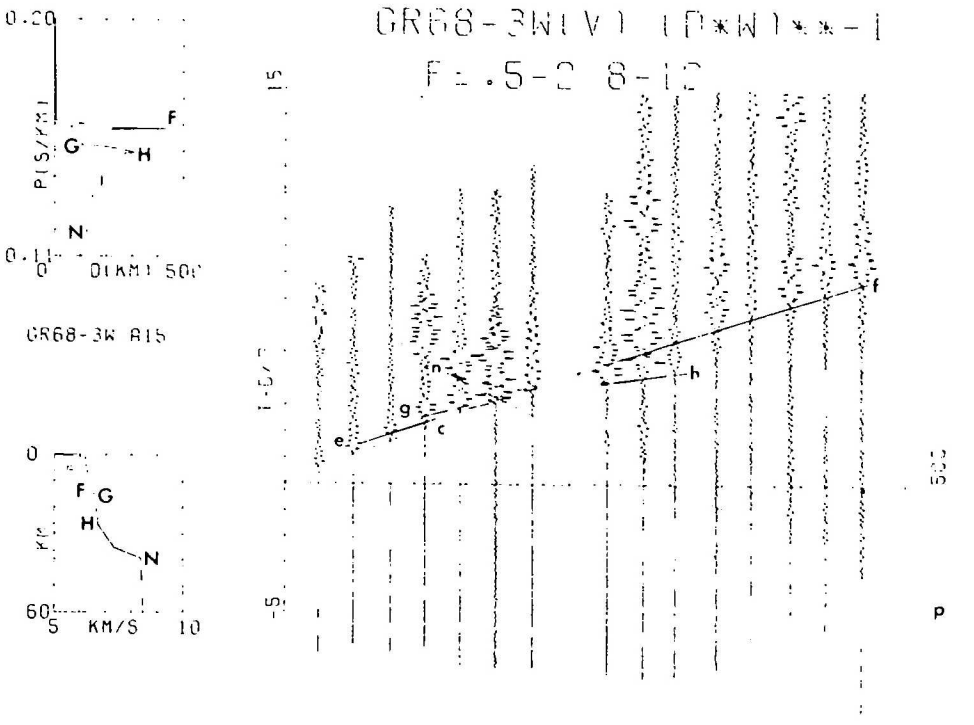

Record section 3W showing, in addition, the travel-time response of model A15.

Figure 15 Observed record section 3W Superior Province/Canada (Berry & Fuchs,1973).

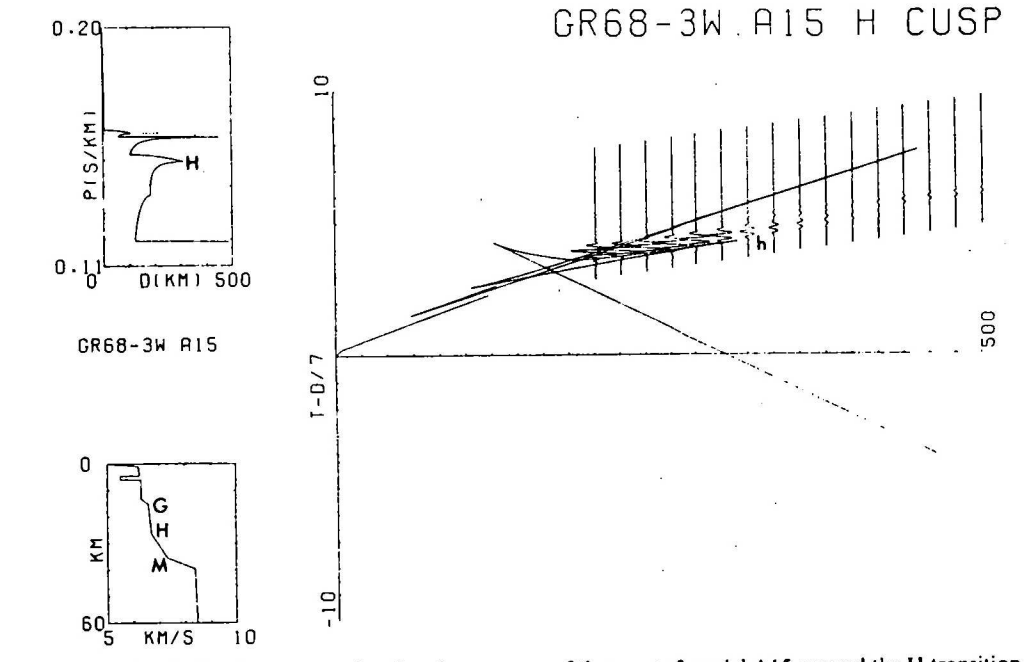

Synthetic seismograms showing the response of that part of model A15 around the H transition.

Figure 16 Model A15 for 3W, travel time curves & synthetic seismograms.

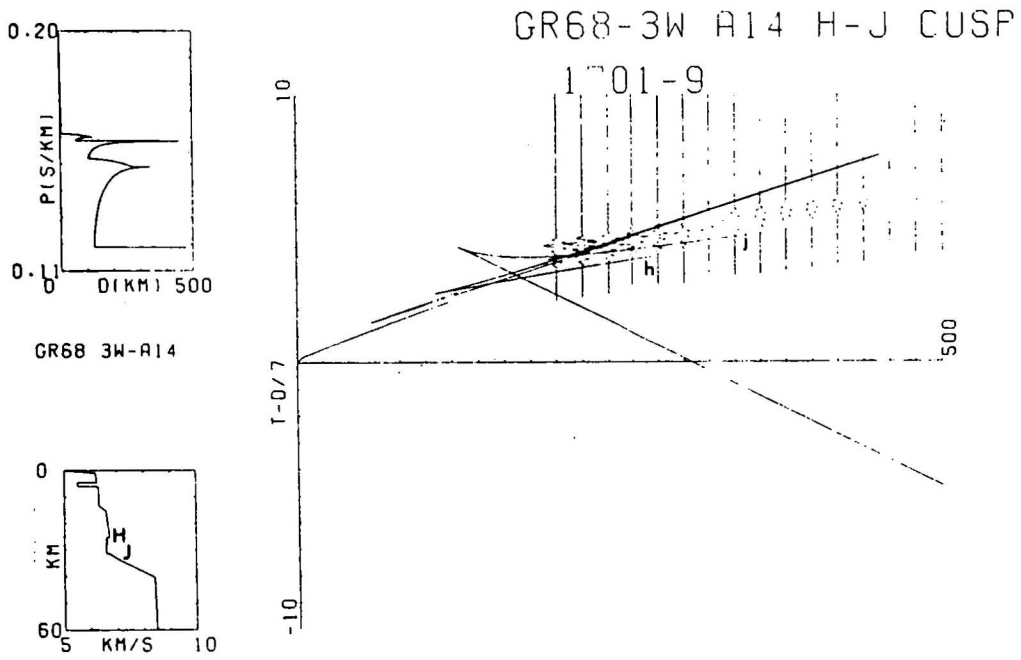

Synthetic seismograms showing the response of a lower low-velocity zone inserted at H in model A15. The model shown here is A14.

Figure 17 Model A16 for 3W, travel time curves & synthetic seismograms, effect of low velocity zone.

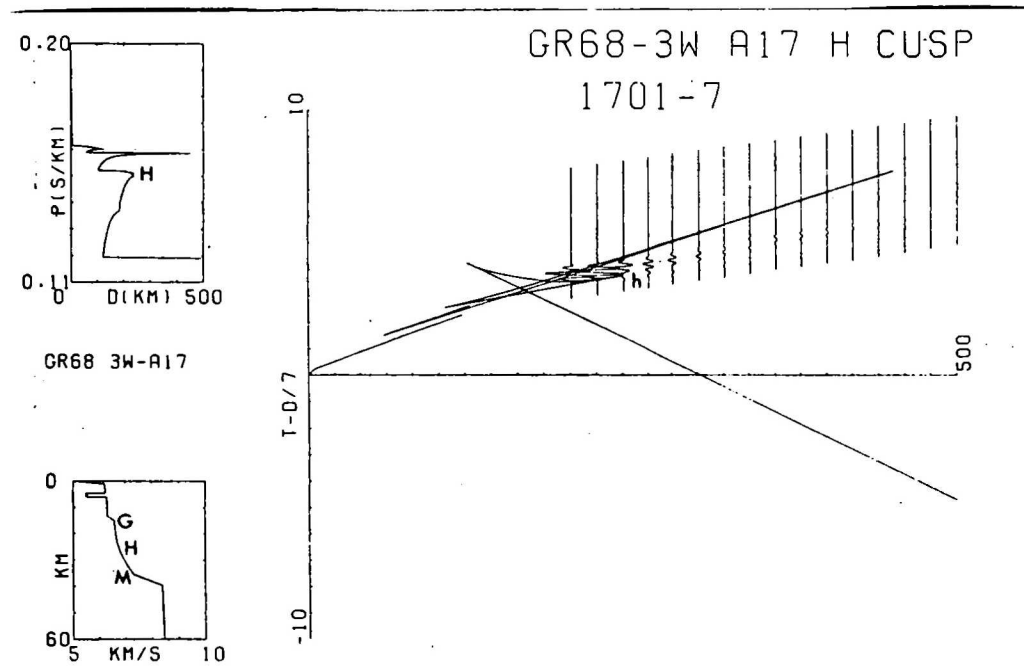

Synthetic seismograms showing the response of a smoothly increasing velocity gradient at H. The model shown is A17.

Figure 18 Model A17 for 3W, travel time curves & synthetic seismograms, bright cusp.

3.1 Cerveny effect

Červený (1961) noted from theoretical investigations that the amplitude maximum for the reflected wave does not occur at the critical distance, as would be expected from geometrical ray theory, but is displaced to larger distances due to the interference of the headwave and the reflected wave, and due to the change in pulse shape of the super-critical reflection. As an interference phenomenon, the shifting of the amplitude maximum of the reflected wave is dependent upon dominant frequency of the incident signal, depth of the reflector, and the velocity contrast at the reflector. The effect increases with decreasing frequency, with decreasing velocity contrast and with increasing depth of the reflector.

See Exercise 3

3.2 Bright cusp

In some explosion seismic studies of the crust, situations occur where large amplitude signals occur on the "outer" cusp of a triplication of a time-distance curve out to the very tip of the cusp, and then fall off abruptly beyond that point. It is relatively easy, by manipulating the gradients in the corresponding layers, to match the theoretical and observed travel times and to place the "outer" cusp at the observed distance. We will consider an example from the Superior Province of the Northeastern Canadian Shield (Berry & Fuchs, 1973). The fit of the observed travel-times to the cusp corresponding to the point H in the depth/velocity curve, and in the ray parameter/distance P(Δ) diagram, both look quite satisfactory. However a synthetic record section for the part H in Fig. 16 shows that the energy does not stop at the cusp h but is actually diffracted beyond the cusp to larger distances with only smooth decay of amplitudes. In our search for an effective means to stop the seismic energy abruptly at a certain distance, we experimented with a low velocity channel in region H. We hoped that as soon as the ray emerging at the cusp h touched the top of the low velocity zone, all energy with higher phase velocity would be dumped into, and lost in, this zone, thus producing an abrupt termination. Fig. 17 shows that the first part of our consideration was correct; the energy entered the low velocity zone. However, the low velocity channel acted as a wave guide, propogating a reverberating signal to much larger distances with smaller amplitude losses than in the simpler structure of Fig. 15 or 16.

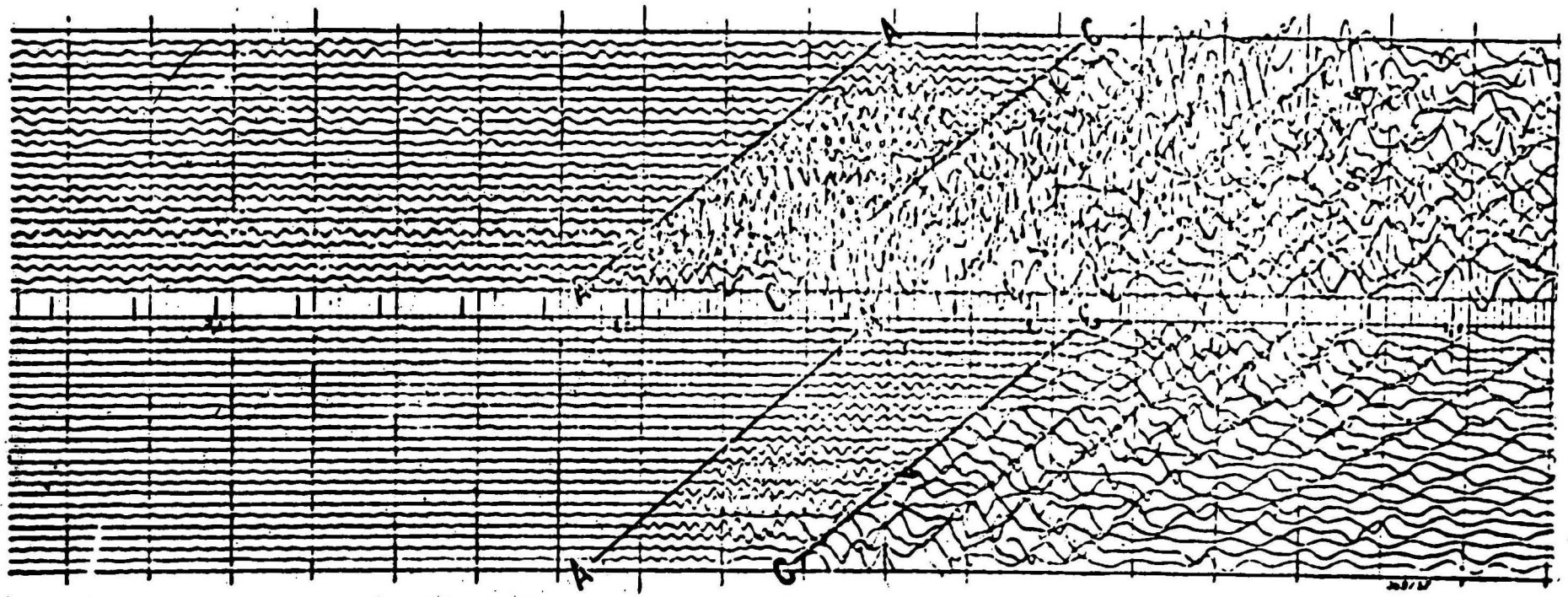

Abb. 3. Seismogramm einer Refraktionslinie in Süddeutschland mit gleichzeitig auftretenden Muschelkalk- und Grundgebirgseinsätzen.

Figure 19 Observed tunnel waves (Krey,1957).

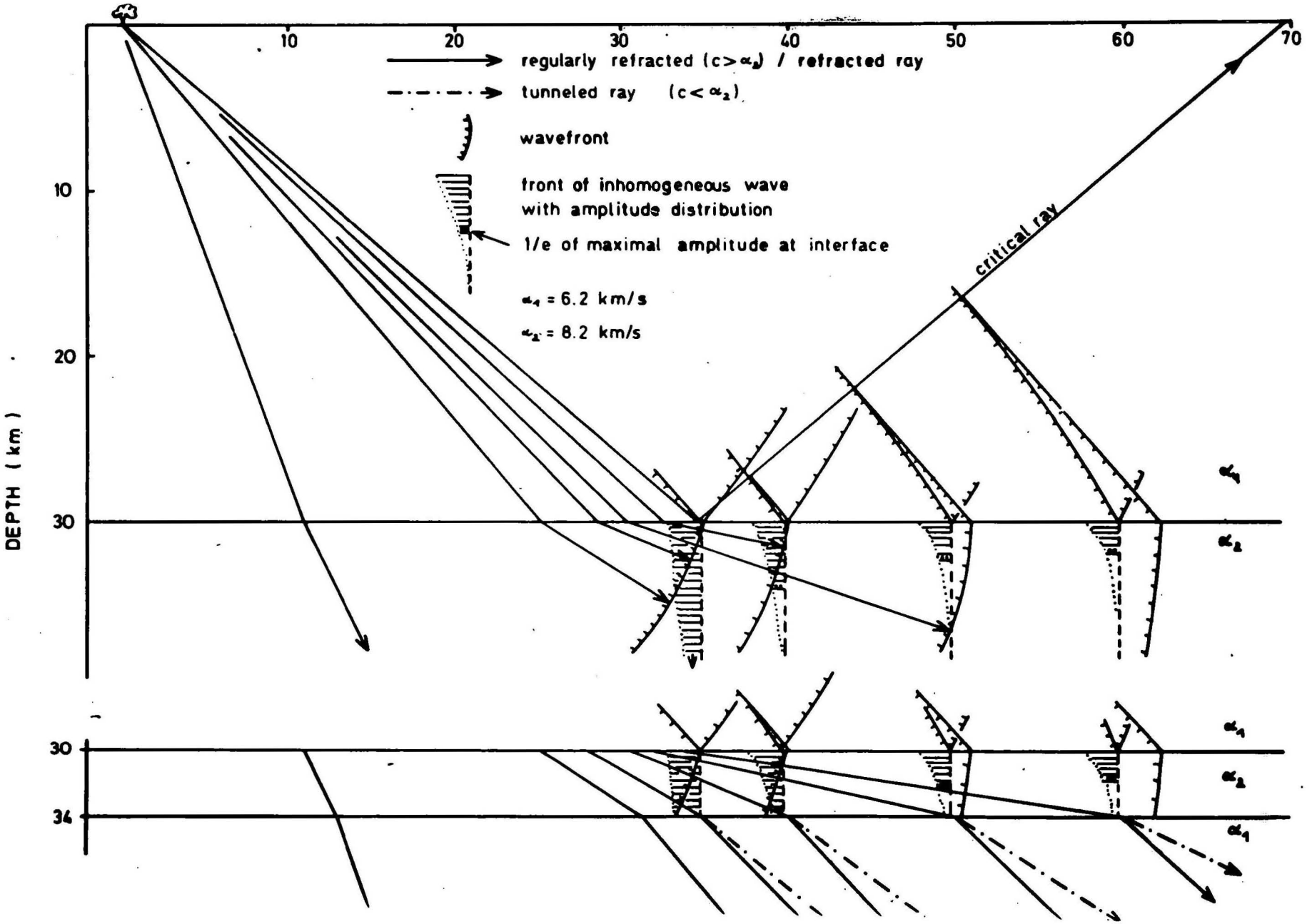

Figure 20 Tunnelling mechanism.

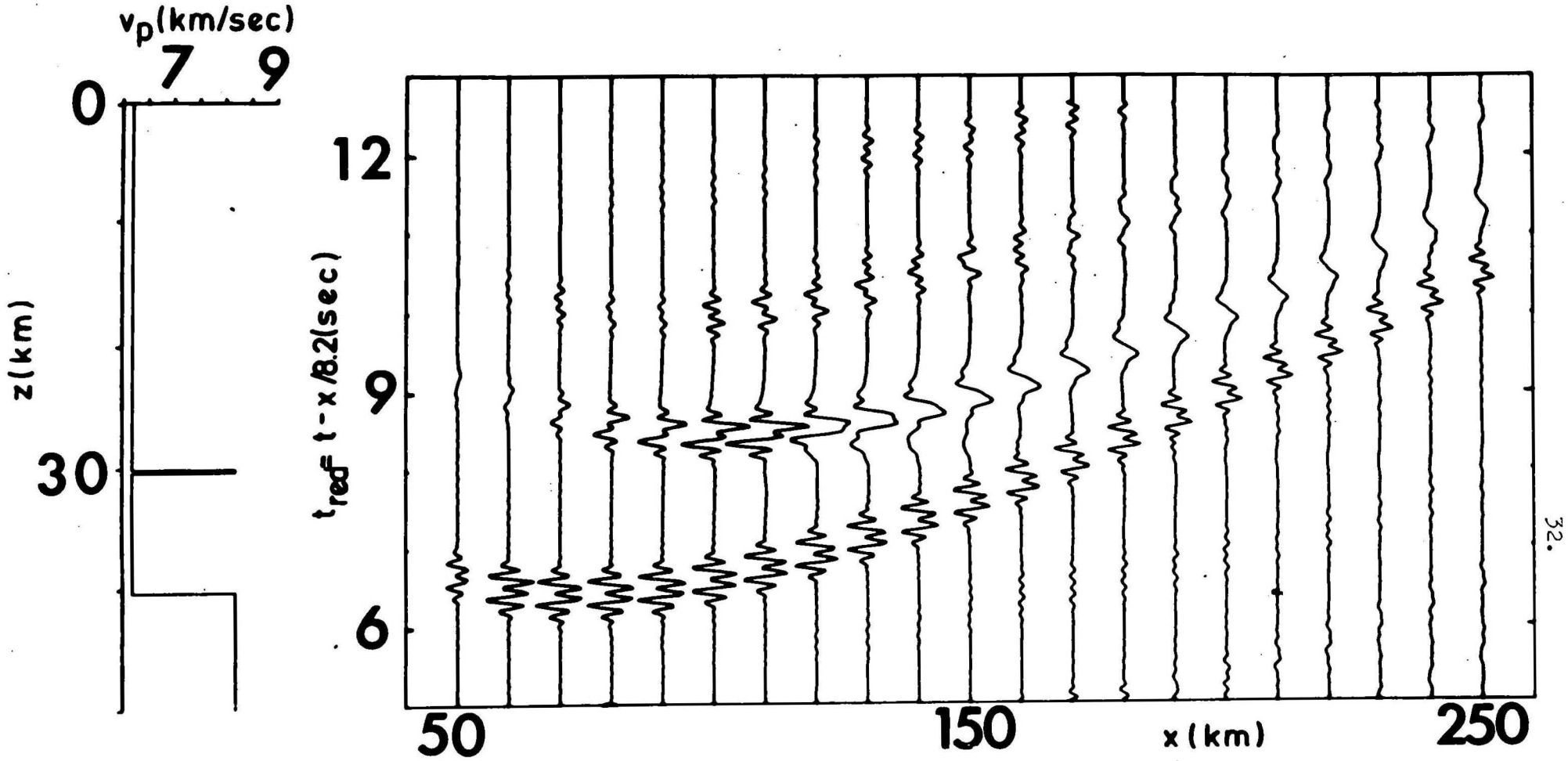

Figure 21 Tunnel wave as a secondary arrival.

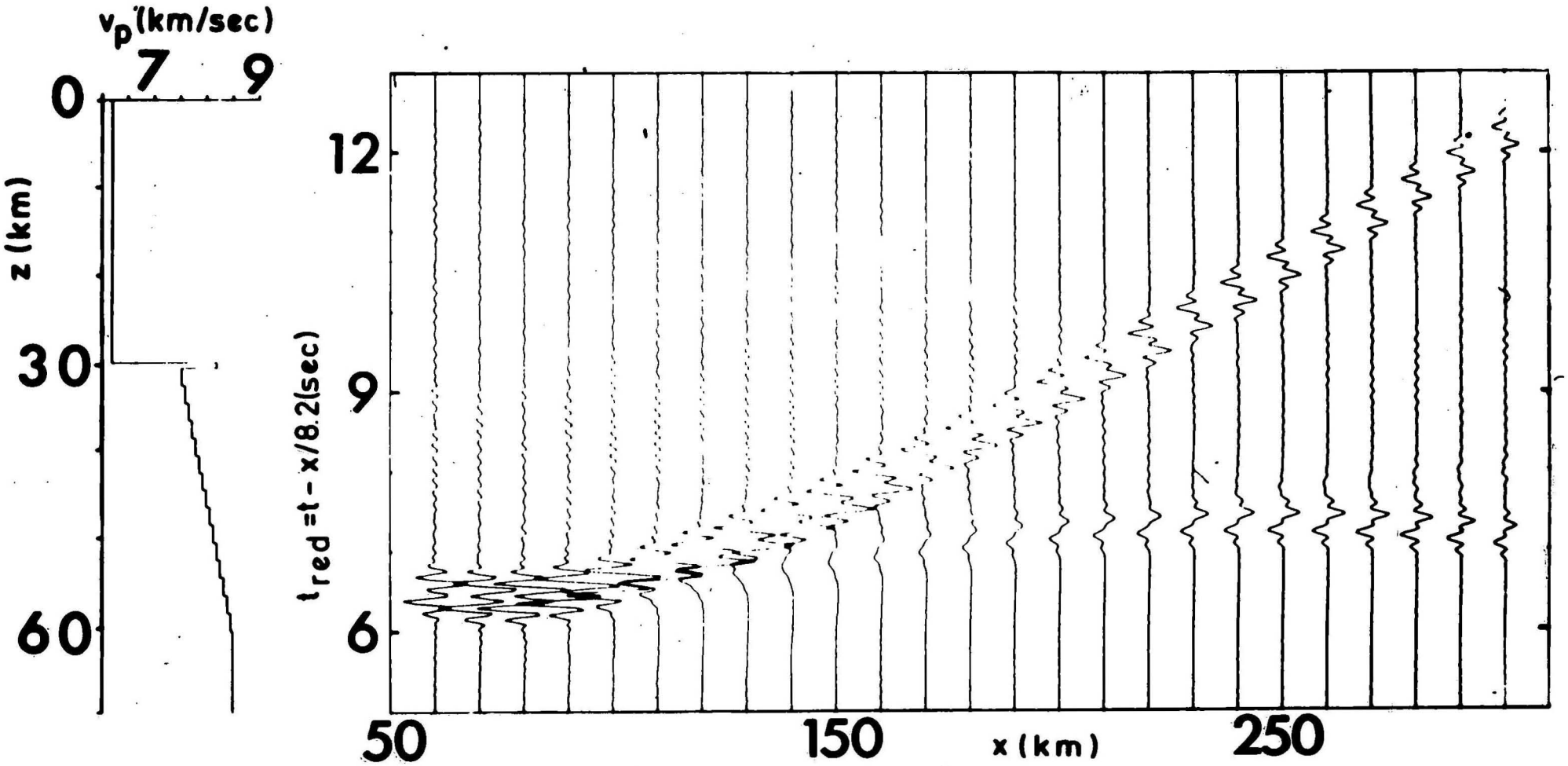

Figure 22 Tunnel wave as a first arrival.

We finally found that the best V(Z) is that which produces in the P(Δ)-diagram a cusp which is smooth and has some finite area, as distinct from the cusp H in figure 15 or 16. The P(Δ) in Figure 18 at the cusp H is a crude approximation to the Bullen condition for a bright outer cusp (Bullen, 1960):

$$\frac{d\Delta}{dp} = 0$$

i.e. at such a cusp neighbouring rays emerge at the same distance.

3.3 Tunnel waves

Seismic tunnel waves, to my knowledge, were first discovered and reported in exploration seismology. Fig. 19 is reproduced from a paper by Krey (1957) which describes the use of low frequency geophones to detect refraction arrivals from a refractor with lower velocity than in a high velocity layer in the overburden:

Low frequency energy is tunnelling through the thin high velocity layer generating the low frequency secondary arrivals, while the high frequencies are propagated as first arrivals in the thin high velocity layer. The mechanism of this tunneling is depicted in Fig. 20:

If a spherical wave is incident from a low velocity medium upon a homogeneous high velocity halfspace at overcritical angle of incidence, an inhomogeneous wave is generated in the lower halfspace and propagates within it, fixed to the point of incidence and reflection. The amplitude of this inhomogeneous wave decays exponentially with depth and the rate of decay depends upon the frequency and the angle of incidence. The higher frequencies are more strongly attenuated than the lower frequencies. Normally these inhomogeneous waves are not noticed at the earth's surface. However, if the high velocity medium is not a halfspace, but a thin layer bounded by a low velocity medium and thin enough that the low frequencies have still sufficient amplitudes, the inhomogeneous wave is converted into a propagating wave again. If this wave is then returned to the surface by reflection or refraction it can be recognised as a low pass filtered wave occurring in regions, at times, and at distances not allowed by geometrical ray theory. The following examples (Fig. 21 and 22) are reproduced from Fuchs & Schulz (1976). In Figure 21 the tunnel waves occur as a secondary low frequency arrival. The secondary arrival is the reflection from the bottom of the low velocity layer below the higher velocity layer. This reflection is broad band in the region where the angle of incidence upon the high velocity is still sub-critical. The energy in the part where the low frequency signals arrive, cannot be explained by geometrical ray theory.

In Figure 22 the tunnel wave is a first arrival by refraction from a transition layer. The low frequency arrival occurs in a distance range where geometrical ray theory would predict a shadow zone formed by the high velocity.

The wave field is similar to that which would be produced without a high velocity layer but a zone of low Q.

4. List of exercises

1) Try to save computer time by increasing Δt from 0.01, 0.02, 0.05 sec and reducing correspondingly the number NPTS in the response time series. All other parameters the same.

Questions:

a) Did you save CPU-time?
b) What happens to the reflected signal?
What is the cause?

2) Computation of synthetic seismograms for
1st Order discontinuity

The travel time curves for the following model are depicted in the accompanying graph:

Layer Thickness (km)	Vp (km/s)	Vs (km/s)	ρ (g/cm^3)
35	6.1	3.52	2.6
	8.0	4.62	3.3

The times have been reduced with V_{red} = 7.0 km/s

Make your own selection of the key parameter settings to compute a synthetic record section in the distance range < 40, 200 km> at intervals of 10 km and try to minimise computer time.

Questions:

a) What time-distance window should be used?
Response duration? Starting time? Reduction velocity?
b) Which frequency window to use? (See Fig. 6)

c) Which velocity window?

d) Which angle increment?

For questions b), c) and d) various groups should try different parameter settings and compare results.

3) Červený effect

The maximum amplitude of the super-critical reflection does not occur at the critical distance but is shifted to a larger distance. The amount of this shift depends, on a number of parameters:

- dominant frequency of source signal
- depth of reflector
- velocity contrast at reflector

3.1) Study the Červený effect by using the model of Exercise 2) using the following source signals

a) Standard signal (already done in Exercise 2)) with duration T_2 = 0.2 sec

b) Double duration T_2 = 0.4 sec

c) Triple duration T_3 = 0.6 sec

All other key parameters should be kept unchanged

3.2) Study the Červený effect by increasing the layer thickness to 45 km. Use standard source signal with duration T_1 = 0.2 sec

3.3) With layer thickness 35 km change the velocity contrast to V_{p_1} = 6.8 and V_{p_2} = 8.0 km/s

5. References

Berry, M.J., and Fuchs, K. (1973). Crustal structure of the Superior and Grenville Provinces of the Northeastern Canadian Shield. Bull. Seism. Soc. Am., 63, 1393-1432.

Bullen, K.E. (1960). Note on cusps in seismic travel times. Geophys. J.R.A.S., 3, 354-359.

Červený, V. (1961). The amplitude curves of the reflected harmonic waves around the critical point. Studia Geophys. Geod., 5, 319-351.

Fuchs, K. (1968). The reflection of spherical waves from transition zones with arbitrary depth-dependent elastic moduli and density. J. Phys. Earth., 16, Special Issue, 27-41.

Fuchs, K. and Müller, G. (1971). Computation of synthetic seismograms with the reflectivity method and comparison with observations. Geophs. J.R.A.S., 23, 417-433.

Fuchs, K. and Schulz, K. (1976). Tunneling of low frequency waves through the subcrustal lithosphere. J. Geophys., 42, 175-190.

Haskell, N.A. (1953). The dispersion of surface waves in multilayered media. Bull. Seism. Soc. Am., 43, 17-34.

Kennett, B.L.N. (1975a). Theoretical seismogram calculation for laterally varying crustal structures. Geophys. J.R.A.S., 42, 579-589.

Kennett, B.L.N. (1975b). The effect of attenuation on seismograms. Bull. Seism. Soc. Am., 65, 1643-1651.

Kind, R. (1976). Computation of reflection coefficients for layered media. J. Geophys., 42, 191-200.

Kind, R. (1978). The reflectivity method for a buried source. J. Geophys., 44, 603-612.

Kind, R. (1979). Extensions of the reflectivity method. J. Geophys., 45, 373-380.

Krey, Th. (1957). Erweiterte Moglichkeiten für die Refraktions-seismik durch die Verwendung von Geophonen mit niedriger Eigenfrequenz (Extended range of applicability for refraction seismic prospecting by the use of low frequency geophones). Geol. Jahrl., 74, 523-530.

Müller, G. (1973). Amplitude studies of core phases. Jour. Geophs. Res., 78, 3468-3490.

Acknowledgements

This workshop was held while the author was visiting Australia under the Australian-European Awards Program. The assistance from the Australian Department of Education is most gratefully acknowledged.

The workshop was suggested by Dr D. Denham and prepared in close contact with him. I am very much indepted to J. Lock and D. Finlayson for reading and improving the manuscript. C. Collins was of great help in the preparation of numerical examples and the exercises. Without the technical assistance of the Bureau of Mineral Resources in preparing the manuscript and the figures the preparation of these notes in such a short time would have been impossible. All this help is gratefully acknowledged.